

# Angle of repose-limited shapes of asteroids

Paul Withers

Lunar and Planetary Laboratory, University of Arizona

Created on December 16, 1999, for Jay Melosh's Surfaces class

## Contents

<b>1</b>	<b>Introduction</b>	<b>3</b>
<b>2</b>	<b>Iterative Search</b>	<b>4</b>
<b>3</b>	<b>Random Walk Approach</b>	<b>5</b>
<b>4</b>	<b>Non-rotating Ellipsoidal Shapes</b>	<b>13</b>
<b>5</b>	<b>Rotating Ellipsoidal Shapes</b>	<b>16</b>
<b>6</b>	<b>Effects of Rotation on Complicated Shapes</b>	<b>21</b>
<b>7</b>	<b>Box Shape</b>	<b>23</b>
<b>8</b>	<b>Future Work</b>	<b>24</b>
<b>9</b>	<b>Conclusions</b>	<b>24</b>

Short title:

**Abstract.** Surface slopes on rotating, axisymmetric, homogeneous bodies are investigated in an attempt to find a shape with its surface slope always at the angle of repose. Ellipsoidal, boxy, and random walk-generated shapes are considered.

## 1. Introduction

Both icy and rocky bodies show a transition in shape with size. Large bodies have oblate ellipsoidal shapes, whereas small bodies have irregular shapes. The ellipsoidal shapes are in hydrostatic equilibrium and are controlled by self-gravity, whereas irregular shapes are controlled by material strength. The transition occurs at around 200 km radius for icy bodies and between 300-500 km radius for rocky bodies, and is accompanied by changes in roughness and in the relation between maximum topographic height and radius [*Slyuta and Voropaev, 1997; Thomas, 1989; Croft, 1992*].

Shape models for well-imaged asteroids and satellites in the strength regime [*Thomas et al., 1994; Thomas et al., 1996; Thomas et al, 1999*] (note that NEAR didn't image Mathilde very well and hasn't published much on the Eros flyby) suggest that slopes on these irregular bodies are almost always less than  $30^\circ$ , a typical angle of repose [*Jaeger and Nagel, 1992*].

In this project I have tried to create axisymmetric shapes which, when given a uniform density, have slopes which are almost always less than  $30^\circ$  and have as large a mean slope as possible. An angle of repose-limited shape will be an endmember for the set of possible asteroid shapes and hence important to study and understand. Section 2 investigates an iterative approach to finding such a shape, Section 3 investigates a large number of possible shapes, generated by a random walk technique, Section 4 investigates ellipsoidal shapes, Section 5 introduces rotation to the ellipsoidal shapes, Section 6 introduces rotation to the shapes used in Section 3, and Section 7 investigates a box-like

shape.

## 2. Iterative Search

In the first homework question of this course, I showed that a non-rotating, homogeneous sphere could be enclosed within a massless surface where the surface was at a constant angle to the local gravity vector. I showed that the limb profile of this surface is given by a logarithmic spiral,  $r = r_0 e^{\phi \tan \theta_r}$ , where  $r$  is the radial coordinate,  $r_0$  is a reference radial coordinate,  $\phi$  is the angular coordinate, and  $\theta_r$  is the angle of repose, here  $30^\circ$ .

This surface is significantly larger than the sphere it encloses. Its long axis has length  $r_0(1 + e^{\pi \tan \theta_r})$ , whereas the sphere's diameter is merely  $2r_0$ . This is a three-fold increase for an angle of repose of  $30^\circ$ .

Filling the generated massless surface with mass and repeating to find a new, axisymmetric enclosing massless surface may iterate to a stable solution with all slopes at the angle of repose. Unfortunately this does not happen — indeed it is not clear that such a shape even exists. After a few iterations, the enclosing massless surface becomes an enlarged version of the shape of the mass within and the iterations continue on this fruitless path indefinitely. The steady state limb profile is roughly similar to a logarithmic spiral but I have not investigated it closely. Figure 1 shows this steady state shape for an angle of repose of  $30^\circ$  on the left, its associated logarithmic spiral on the right. The initial sphere would be shown as a semicircle 20 units in diameter in this Figure. The increase in size from enclosed mass to enclosing surface increases as the

angle of repose increases. This shape may have some interesting properties but it did not seem helpful in solving the problem of angle of repose-limited asteroidal shapes.

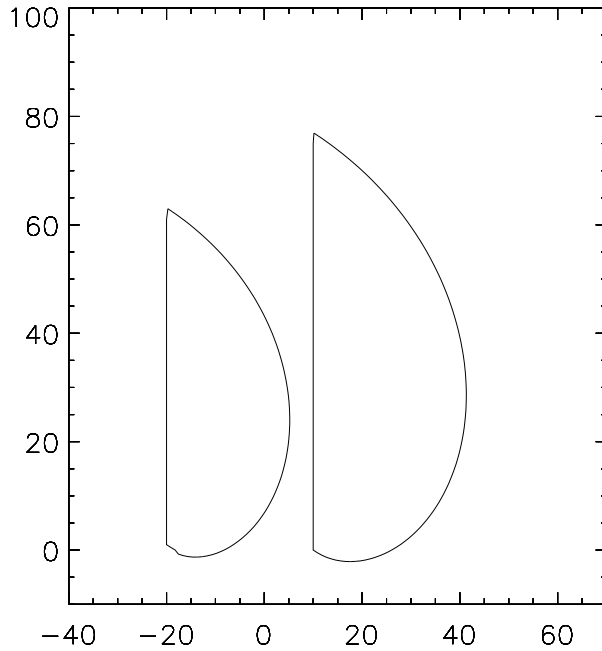


**Figure 1.** *Steady state solution (left) and logarithmic spiral (right), as discussed in Section 2.*

### 3. Random Walk Approach

A different, brute force, approach to the problem is to generate lots of possible limb profiles and see if any of them, when used to define an axisymmetric, non-rotating, homogeneous body, have slopes which are always at the angle of repose.

There are many ways to generate limb profiles and finding the most useful one was one of the more challenging parts of this project. The only way I could think of to consider every possible limb profile was to start off a lot of two dimensional random

walks. Stop the walks after a suitably large number of steps. Try to draw an axis between the start and end points. If this line crosses the random walk, discard this random walk. If it doesn't and the random walk doesn't cross over itself, both of which will be rare for random walks with a large number of steps, then this random walk can be used as a possible limb profile.

However, to get an interesting shape requires many steps in the random walk. Getting a feasible shape from a many-step random walk requires many attempts. I did not have the patience or the computing power to generate huge numbers of shape models, of which only a few would be usable.

Instead I constrained my random walk to generate only usable limb profiles. In doing this I also prevented my random walk from producing certain features which it is entirely plausible to have in a real asteroid limb profile.

- Begin at origin of coordinates.
- Move horizontally outward 1 unit from what will be the vertical symmetry axis.
- If just moved horizontally, continue 1 unit in same direction or move vertically upwards 1 unit, with equal probabilities of moving either way.
- If just moved vertically upwards, move 1 unit horizontally in the same direction as most recent horizontal move, or move 1 unit vertically upwards, or move 1 unit horizontally in the opposite direction to the most recent horizontal move. Probability of flipping horizontal direction is small, other two probabilities are

equal. The probability of flipping horizontal direction can be varied from one simulation to the next.

- Once you have flipped horizontal direction, probability of further flips is zero.
- Stop when walk returns to vertical symmetry axis.
- To reduce number of right-angled vertices and simplify code, define shape only by the outermost horizontal point for a given vertical coordinate. Add in on-axis points at top and bottom of shape if necessary.
- Regrid to be defined by 20 pairs of coordinates, spaced equally in the vertical direction and including the two points on axis at the top and bottom of the shape.
- Different shapes are therefore defined by the 18 off-axis horizontal coordinates.

A few example shapes produced by this method are shown in Figure 2.

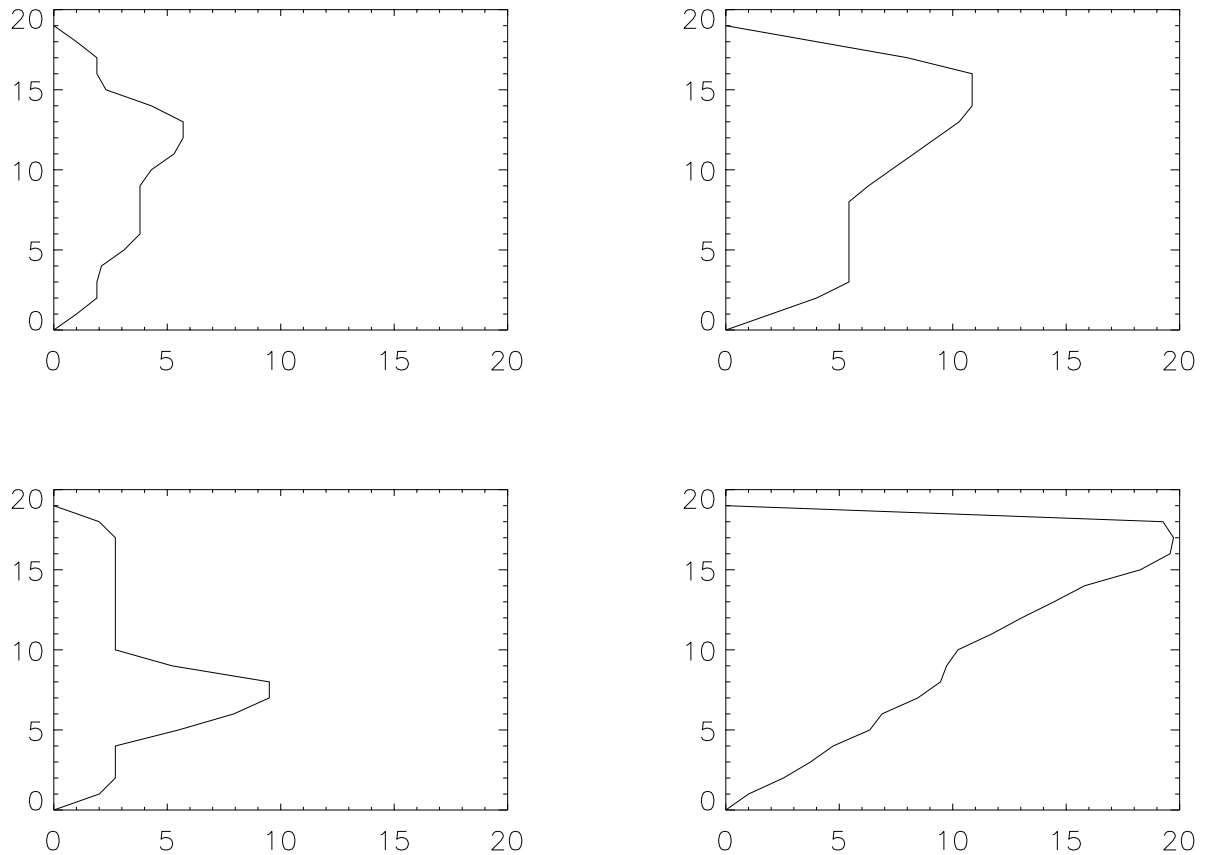


**Figure 2.** *Pre-stretched shapes produced by the algorithm discussed in Section 3.  $P_{flip} = 1/7$  (top left),  $1/11$  (top right),  $1/15$  (bottom left), and  $1/21$  (bottom right).*

The major problems with this model for generating possible shapes are that you can only move monotonically outwards from the axis, then monotonically back inwards, and that you can only move monotonically upwards from the starting point. The first problem can easily be fixed by allowing the direction to flip without restrictions. The second problem must remain, otherwise my code will be confused when it has three horizontal positions for the surface at a single vertical position. However it could be

fixed without much difficulty.

The tendency to have surfaces at  $45^\circ$  to the axis due to the equal probabilities of moving vertically or horizontally is corrected after the shape is generated when a single stretch factor is applied in the horizontal direction.

The two free parameters in this model are the probability of flipping horizontal direction and the horizontal stretch factor. The probability of flipping horizontal direction was either  $1/7$ ,  $1/11$ ,  $1/15$ , or  $1/21$ . The horizontal stretch factor was either  $1/5$ ,  $1/2$ ,  $1$ ,  $2$ , or  $5$ . Ten simulations for each pair of parameters were performed, yielding a total of 200 shapes.

Between each adjacent pair of coordinates the directions of the local gravity vector and of the local surface normal on the surface of the axisymmetric, non-rotating, homogeneous body were calculated. These directions were used to find the slope of the surface with respect to gravity.

Shapes with greater than 3 of the 19 slope values larger than  $30^\circ$  were rejected as being too steep over too large a fraction of their surface. A few slopes exceeding the angle of repose were allowed to remain, as shape models for real asteroids see a small number of such slopes. Over three-quarters (153) of the 200 simulations were rejected.

Considering only the 47 simulations remaining, and neglecting the few points with slopes exceeding the angle of repose, I did a rough statistical investigation of the data, performing linear least-squares fits between:

1. mean slope and standard deviation of slope

2. axial ratio, a common measure of asteroid shape, and mean slope
3. “chest length” and mean slope

where “chest length” is the vertical separation of the “waist” (point of maximum horizontal distance from axis) and the closest end of shape. A rough goodness-of-fit measure is the ratio of the uncertainty in the fitted gradient to the value of the fitted gradient — this is used primarily because it falls naturally out of my code. Values of this parameter for the three comparisons are 0.09, -0.20, and 3.87 respectively. Eyeballing the data, I find only the first fit, Figure 3, convincing. The second is strongly affected by a few extremal data points. Removing 3 of the 47 simulations changes my parameter from -0.20 to 1.06.

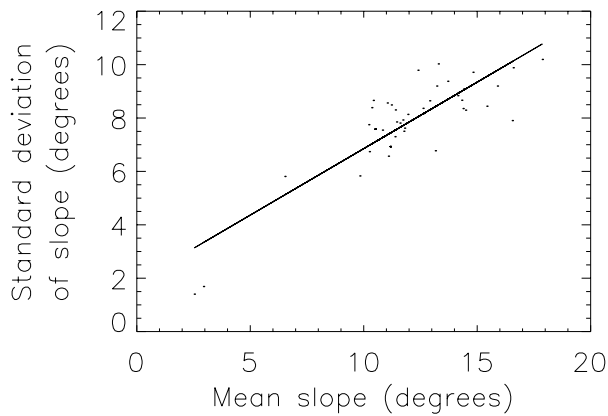


**Figure 3.** *Correlation between mean slope and standard deviation of slope for unrejected shapes.*

I conclude that in my 47 realistic simulations of asteroid shapes there is no

correlation in 2) or 3) but there is a good correlation in 1). There are too few accurate shape models for asteroids, and I don't have my hands on the numbers for the ones that do exist, for me to see if these results are reproduced in real asteroids. I would also prefer to do any comparisons with a better statistical method and more than 47 simulations.

Five of the 47 simulations had mean slopes of greater than  $15^\circ$  after neglecting the few points with slopes exceeding the angle of repose.

The shape and local gravity vectors of one of these are shown in Figure 4. Length of arrow is proportional to strength of local gravity, crossed end of arrow indicates direction of gravity.

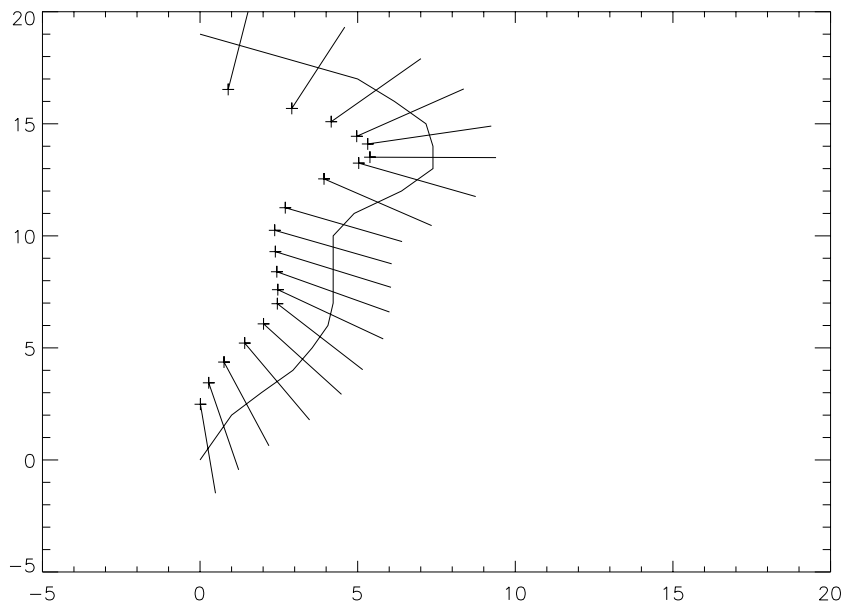


**Figure 4.** *Example shape and direction of local gravity. Horizontal stretch factor =  $1/2$ ,  $P_{flip} = 1/15$ .*

Returning to the five shapes, their properties and the parameters used to generate

them are tabulated below:

**Table 1.**

Probability of Flipping Horizontal Direction	Horizontal Stretch Factor	Chest length / Along-axis length	Mean Slope (degrees)	Standard deviation of slope (degrees)	Along-axis length / Diameter at waist
1/21	1	3/20	16.6	7.9	0.48
1/11	1	6/20	16.6	9.9	0.88
1/11	1/2	6/20	17.9	10.2	2.43
1/11	2	3/20	15.4	8.4	0.44
1/15	1/2	7/20	15.9	9.2	1.29

The only comment with anything approaching statistical significance that I am prepared to make about the parameters which gave these five shapes is that a probability of flipping of 1/11 seems more likely to generate realistic shapes with large mean slopes than the other possible options.

This sample size is so small (5) that it is not sensible to try to study trends within the sample; we can only look at the sample as a whole. The waist tends to occur away from both the poles and the equator. There is only a small range in values for mean slope and standard deviation of slope. A wide range of axial ratios are present.

None of the 200 simulations have slopes which are almost always less than  $30^\circ$  and a mean slope of over  $18^\circ$ . This suggests that this approach is not very good at finding angle of repose-limited asteroidal shapes

Attempts to use some of the more interesting shapes in this section in the work of

section 2, by using these shapes (rather than a circle) as a starting point for the limb profile, were unsuccessful. A slightly deformed approximation to the roughly logarithmic spiral was produced, again several times larger than the original shape, which quickly iterated to the same steady state as in section 2.

#### **4. Non-rotating Ellipsoidal Shapes**

The disappointing results of the previous section led me to investigate some simpler shapes, and see if they were any more successful. Axisymmetric ellipsoids seemed like a good place to start as many asteroids have been modelled as ellipsoids (not necessarily figures of hydrostatic equilibrium as appropriate to large bodies in Section 1) and the shape of an axisymmetric ellipsoid is completely defined by one parameter, the ratio of its axes.

**Table 2.**

Along-axis length / Diameter at waist	Mean Slope (degrees)	Standard deviation of slope (degrees)	Maximum slope (degrees)
5	23.0	13.0	40.0
2	13.8	7.2	21.2
1	2.8	2.0	6.1
0.5	10.4	4.7	15.5
0.2	24.2	11.3	38.1
0.25	21.2	9.8	32.8
0.33	17.0	7.7	26.1
0.29	19.3	8.7	29.4

The “0.2” and the “5” ellipses are identical, as are the “0.5” and the “2” ellipses. These same shapes will be used in the next section with rotation, which will distinguish between them. Differences between the supposedly identical cases are due to different numbers of mass points contained within them. The “1” ellipse is a sphere and should have a slope which is everywhere zero. These results suggest that an error on the order of  $5^\circ$  is present in my slope calculations. It is easy to reduce this by using a finer grid. For the present work, it is acceptable.

It is clear that an ellipsoidal shape, with “Along-axis length / Diameter at waist”  $\sim 0.3$ , as in Figure 5, will have a mean slope greater than the most favourable case in

Section 3 without any slopes exceeding the angle of repose.

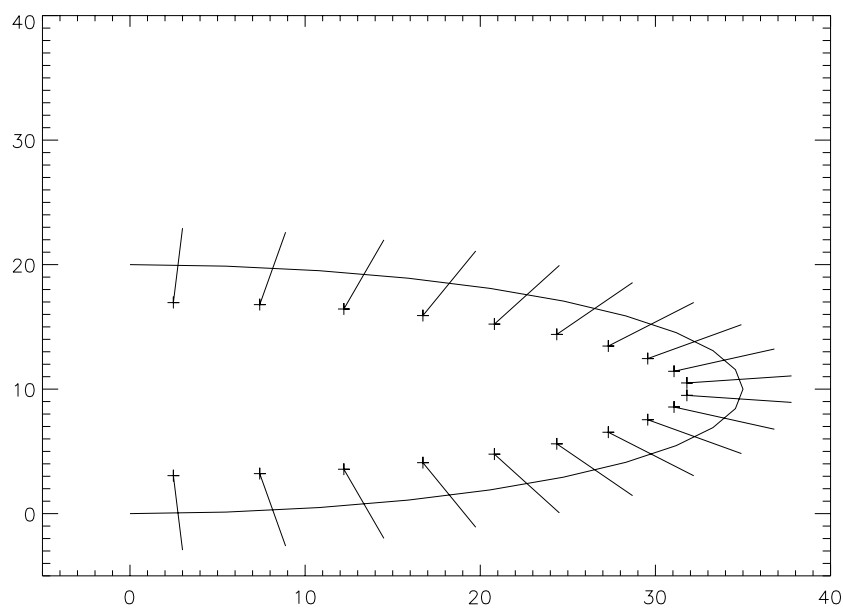


**Figure 5.** *Ellipsoidal shape with mean slope  $\sim 20^\circ$  and maximum slope less than  $30^\circ$ .*

This suggests that my random walk method has done very poorly at generating interesting shapes for me to study. I would be amazed if some analytical discussion of what I have tried to do in this section is not present in the literature. If it doesn't exist, I should go ahead and do it, because I can see it being very useful. Had I worked on this section a few weeks earlier than I did, I would have concentrated my attention on this aspect of the project. Having other things to do now, I will just note that the results for an ellipsoidal shape are simply a function of the axial ratio.

## 5. Rotating Ellipsoidal Shapes

Most asteroids rotate with periods on the order of a few hours. The subsequent centrifugal force affects the direction of local “gravity”. Henceforth “gravity” refers to any force on a object which is proportional to its mass, not just gravitational effects. Like true gravitational effects, rotational effects on the slope are size independent. In an axisymmetric, homogeneous body, the additional effects of rotation depend solely on the rotational parameter,  $\omega^2/(G\rho)$ , where  $\omega$  is the angular frequency of the asteroid’s rotation,  $G$  is the gravitational constant, and  $\rho$  is the density of the asteroid.

Letting  $x$  be the direction perpendicular to the axis of rotation and  $z$  be the direction parallel to the axis of rotation, the gravitational acceleration experienced by a surface particle at  $(x^*, z^*)$  on is given by:

$$g_x = \sum \frac{G\rho d^3V(x_i - x^*)}{|(r_i - r^*)|^3} \quad (1)$$

and similarly for  $g_z$  in the absence of rotation, where  $d^3V$  is the size of the volume element within the body,  $(x_i, z_i)$  is the position of the volume element, and the sum is carried out over all volume elements within the body.

With the introduction of rotation,  $g_z$  is unchanged, and  $g_x$  is increased by the addition of  $\omega^2 x^*$ . Defining  $R$  as a measure of length and  $\rho_0$  as a measure of density,  $g_x$  changes to:

$$g_x = G\rho_0 R \left( \sum \frac{(\rho/\rho_0)(d^3V/R^3)((x_i - x^*)/R)}{|(r_i - r^*)|^3/R^3} + (\omega^2/G\rho_0)(x^*/R) \right) \quad (2)$$

Defining  $R$  as the size of a volume element, letting  $\rho_0 = \rho$ , and redefining all lengths in terms of  $R$  reduces this equation to:

$$g_x = G\rho R \left( \sum \frac{x_i - x^*}{|(r_i - r^*)|^3} + (\omega^2/G\rho)x^* \right) \quad (3)$$

It is now straightforward to include rotation in my code.

Increasing rotational effects will cause the local gravity vectors to rotate towards a direction outward from and perpendicular to the rotation axis. Any slopes greater than  $90^\circ$  will have any loose material on them flowing directly out and away from the asteroid, rather than rolling down a slope.

Using a density of  $3000 \text{ kg m}^{-3}$ , the rotational parameter,  $\omega^2/(G\rho)$ , has a value of 1000 for a period of 10 minutes, 10 for a period of just over 1 hour, and 0.1 for a period of just over 10 hours. Only one asteroid with a period less than 2 hours has been identified. It has a period of 10 minutes. Periods of 100 hours or greater would have a negligible effect on the local gravity.

A rotational parameter of 0.1 has a tiny effect and its results are not of interest. A rotational parameter of 10 has a significant effect, making the mean slope greater than  $90^\circ$  for the first five ellipsoidal shapes in Table 2. A rotational parameter of 1000 completely overwhelms true gravitational effects by rotational effects. These first runs serve to highlight the range of interest for the rotational parameter. Next, I used values of 0.3 and 1.0 for the rotational parameter.

**Table 3.** Rotational parameter = 0.3

Along-axis length / Diameter at waist	Mean Slope (degrees)	Standard deviation of slope (degrees)	Maximum slope (degrees)
3.33	24.5	13.8	42.5
2.5	19.7	10.6	31.9
2.22	19.4	9.9	29.8
2	15.7	8.2	24.1
1	4.4	3.2	9.2
0.5	7.6	3.4	11.2

Examining a small but non-negligible rotational parameter of 0.3 shows that once again we have an ellipsoidal shape with a mean slope of nearly  $20^\circ$  but a maximum slope of less than  $30^\circ$ .

**Table 4.** Rotational parameter = 1.0

Along-axis length / Diameter at waist	Mean Slope (degrees)	Standard deviation of slope (degrees)	Maximum slope (degrees)
5	31.4	18.3	58.3
2	20.8	10.8	32.1
1.67	19.5	10.2	31.1
1.54	17.8	9.8	28.8
1.43	15.8	8.8	25.4
1.25	13.5	8.0	22.8
1	10.0	6.3	18.3
0.5	2.4	1.6	5.7
0.2	5.6	5.5	18.0

With an increased value of the rotational parameter we still have an ellipsoidal shape with a mean slope of nearly  $20^\circ$  but a maximum slope of less than  $30^\circ$ .

**Table 5.**

Rotational Parameter	“Along-axis length / Diameter at waist” that gives largest mean slope without any slopes exceeding $30^\circ$  (using only examples from Tables 2,3, and 4)	Mean Slope  (degrees)
0	0.3	19
0.3	2.2	19
1.0	1.5	18

It seems likely that there is a continuous trend of ellipsoidal shapes having mean slopes not much less than  $20^\circ$  but maximum slopes less than  $30^\circ$  as you increase the rotational parameter from 0 to some value between 1.0 and 10. It is interesting that the “Along-axis length / Diameter at waist” of the “best” ellipse does not change monotonically as the rotational parameter is increased. There is lots of parameter space still to explore here, with only the ellipse shape and rotational parameter controlling the solution. If this hasn’t been done, it’s worth doing and an analytical solution may be possible.

The rotation periods covered here range from infinitely slow rotation to a period of just over 10 hours for a density of  $3000 \text{ kg m}^{-3}$ . The shortest period can be reduced by more simulations and it appears likely that many asteroidal densities and rotational periods will fall within the region in which there is an ellipsoidal shape model with mean slopes not much less than  $20^\circ$  but maximum slopes less than  $30^\circ$ .

## 6. Effects of Rotation on Complicated Shapes

I look now at the effects of rotation on the results of Section 3.

**Table 6.**

Rotational Parameter	Number of unrejected shapes (out of 200)	Number of unrejected shapes with mean slopes greater than $15^\circ$ (out of 200)
0	47	5
0.1	50	6
0.3	71	10
1.0	67	4
3.0	0	0

Two shapes were unrejected for the four smallest rotational parameters tabulated above and many shapes were unrejected for two or three values of the rotational parameter. Figure 6 shows how the slopes on one of the two afore-mentioned shapes

change with increasing effects of rotation.

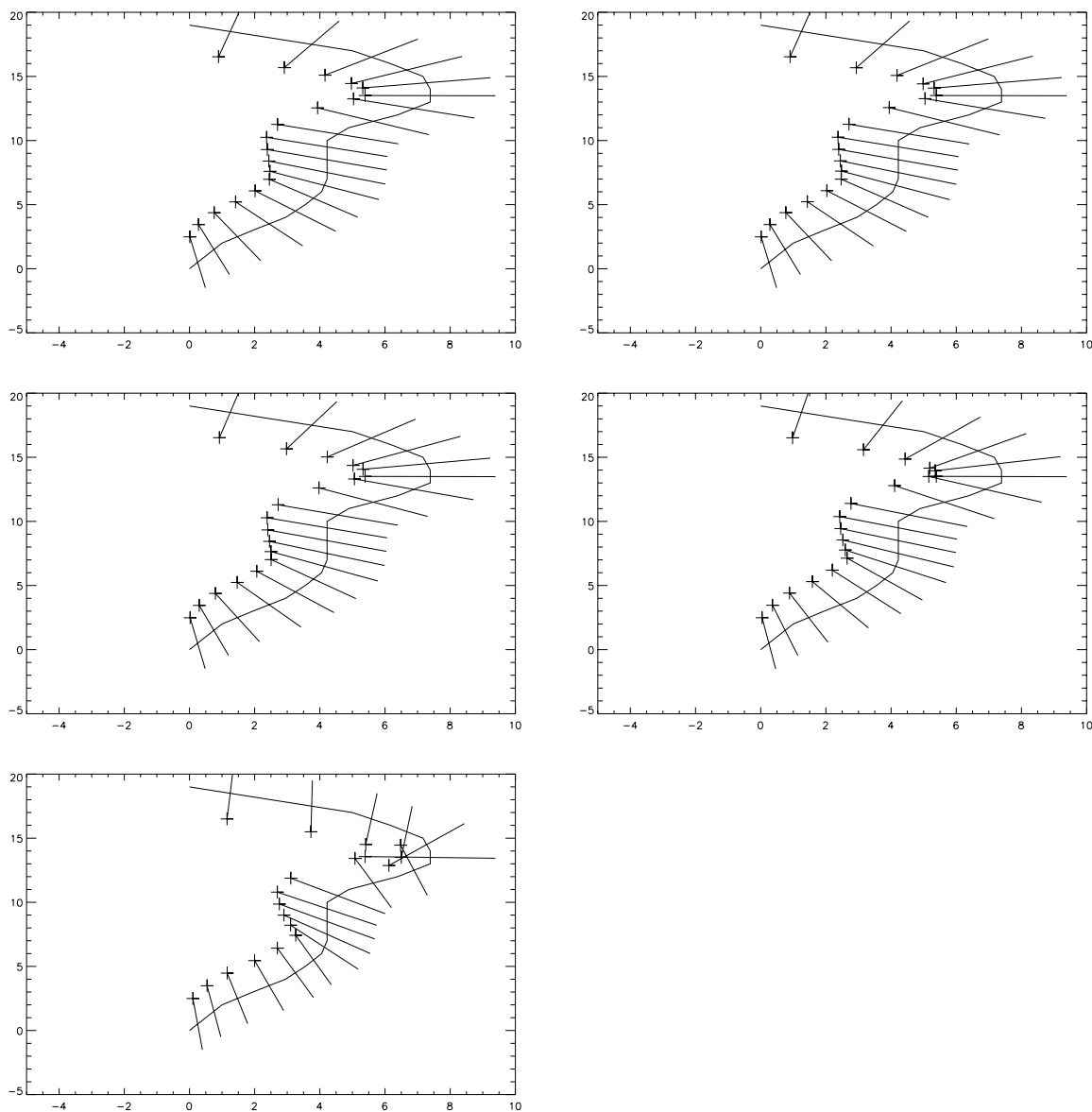


**Figure 6.** Example shape with  $P_{flip} = 1/15$ , horizontal stretch factor =  $1/2$ . Direction of gravity is shown as in Figure 4. Rotational parameter = 0 (top left), 0.1 (top right), 0.3 (middle left), 1.0 (middle right), and 3.0 (bottom). Observe how the direction of gravity changes in response to the increased rotation  
Lots of work is possible examining the changing properties of unrejected shapes,

such as the largest mean slope in these simulations for a given rotational parameter. I shall limit myself to noting that the “best” ellipsoidal shape still seems to have a larger mean slope than the “best” shape generated by a random walk and that the transition from many to few unrejected shapes will be interesting.

## 7. Box Shape

Another simple shape worth investigating after the interesting results of the ellipsoidal shape is a symmetrical trapezium. See Figure 7. This shape has two free parameters,  $b/a$  and  $c/a$ . Rotation axis is side  $a$ .

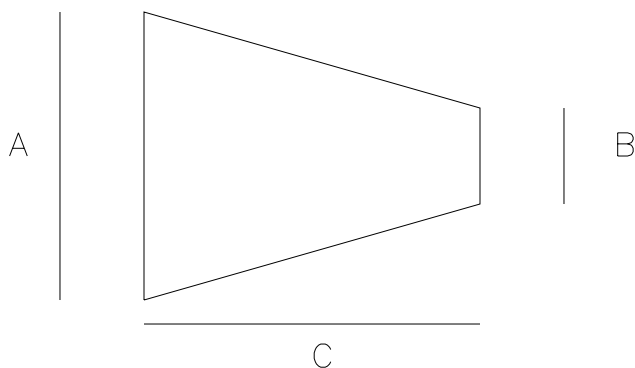


**Figure 7.** *Box shape for use in Section 7.*

Values of  $b/a$  of 0.2, 0.5, and 0.8,  $c/a$  of 0.2, 0.5, and 1.0, and the rotational parameter of 0, 0.3, and 1.0 were used in 27 simulations. Results were much less interesting than for the ellipsoids. Only a handful of simulations had maximum slopes of less than  $30^\circ$ , and none of those had mean slopes greater than  $15^\circ$ . It appears that smooth shapes (ellipsoids) give better results than shapes with sharp vertices and straight edges (boxes). Again, an analytical description should be possible, but it is not

clear that it would be very useful.

## 8. Future Work

Where to begin? There are many interesting ideas deserving of further study that are highlighted by this project. Improved random walk shape models and finer gridding will ensure that every possible shape is examined, the steady state profile found in Section 2 may have some interesting properties, and the work on ellipsoids in Sections 4 and 5 looks as if a small amount of further work could yield great understanding. Triaxial ellipsoids, closer to the shapes of real asteroids, would be a natural extension. Some comparisons with real asteroidal shape models would be useful for suggesting ways to evaluate the shape models, such as their surface roughness. To summarize, once a shape model is created, you can do many interesting things with it. The trick is generating every possible shape.

## 9. Conclusions

It is not clear that a shape exists for an axisymmetric, non-rotating, homogeneous body such that its surface slope is everywhere at the angle of repose. Nevertheless, examining shapes which come close to this ideal provides an important endmember for the family of possible asteroidal shapes (and shapes of small satellites and possibly cometary nuclei.) Surprisingly, a random walk-generated shape proved less successful in this respect than a simple ellipsoid shape. Improved random walk-generated shapes may change this situation. For rotational and density parameters appropriate to many

asteroids, it was found that an ellipsoidal shape could provide a mean slope of nearly  $20^\circ$  with a maximum slope of less than  $30^\circ$ . Angular box shapes were spectacularly unsuccessful.

## References

- Croft, S. K., Proteus: Geology, Shape, and Catastrophic Destruction, *Icarus*, *99*, 402-409, 1992.
- Hartmann, W. K., Moons and Planets, 2nd Ed., 1983.
- Jaeger, H. M., and S. R. Nagel, Physics of the Granular State, *Science*, *255*, 1523-1531, 1992.
- Johnson, T. V., and T. R. McGetchin, Topography on Satellite Surfaces and the Shape of Asteroids, *Icarus*, *18*, 612-620, 1973.
- Slyuta, E. N., and S. A. Voropaev, Gravitational Deformation in Shaping Asteroids and Small Satellites, *Icarus*, *129*, 401-414, 1997.
- Thomas, P. C., The Shapes of Small Satellites, *Icarus*, *77*, 248-274, 1989.
- Thomas, P. C., Gravity, Tides, and Topography on Small Satellites and Asteroids: Application to Surface Features of the Martian Satellites, *Icarus*, *105*, 326-344, 1993.
- Thomas, P. C., and 7 colleagues, The Shape of Gaspra, *Icarus*, *107*, 23-26, 1994.
- Thomas, P. C., and 6 colleagues, The Shape of Ida, *Icarus*, *120*, 20-32, 1996.
- Thomas, P. C., and 8 colleagues, The Small Inner Satellites of Jupiter, *Icarus*, *135*, 360-371, 1998.
- Thomas, P. C., and 11 colleagues, Mathilde: Size, Shape, and Geology, *Icarus*, *140*, 17-27, 1999.

---

Paul Withers Lunar and Planetary Laboratory, University of Arizona, Tucson, AZ  
85721. (e-mail: withers@lpl.arizona.edu)

Received \_\_\_\_\_

Created December 16, 1999, using GRL agums style files